

# ROLE OF MACROPHAGIC HIFs IN THE RESOLUTION OF INFLAMMATION DURING SKELETAL MUSCLE REGENERATION: A COMBINED *IN VITRO*, *EX VIVO* AND MULTIMODAL MRI INVESTIGATION

JULIEN GONDIN<sup>1</sup>, GUILLAUME DUHAMEL<sup>1</sup>, MARINE THERET<sup>2</sup>, KATARINA PEGAN<sup>3</sup>, CAROLE PEYSSONNAUX<sup>2</sup>, SYLVAIN CUVELLIER<sup>2</sup>, BENEDICTE CHAZAUD<sup>2</sup>, DAVID BENDAHAN<sup>1</sup>, and REMI MOUNIER<sup>2</sup>

<sup>1</sup>Aix-Marseille University, CNRS, CRMBM UMR 7339, MARSEILLE, France, <sup>2</sup>INSERM, U1016; CNRS, UMR8104; Université Paris Descartes, Institut Cochin, PARIS, France, <sup>3</sup>Institute of Pathophysiology, Faculty of Medicine, University of Ljubljana, LJUBLJANA, Slovenia

**Target audience:** physiologists; physiopathologists, experts in the field of skeletal muscle function

**Purpose:** The critical role of macrophages (MPs) and the corresponding inflammatory response associated to the muscle repair process has been recently highlighted<sup>1</sup>. Several studies have demonstrated that HIF-1 $\alpha$  could play a key role in inflammation<sup>2,3</sup>. It has been recently claimed that myeloid HIF-1 $\alpha$  was essential for skeletal muscle regeneration after a soft trauma<sup>4</sup>. However, the deletion of HIF-1 $\alpha$  in MPs actually induced only a short delay at the onset of the repair process. Furthermore, the resolution of inflammation, which is indispensable for skeletal muscle regeneration<sup>5</sup>, was not investigated. In the present study, we aimed at carefully addressing the role of myeloid HIFs in the resolution of inflammation during skeletal muscle regeneration on the basis of *in vitro* and *ex vivo* experiments combined to *in vivo* multimodal magnetic resonance imaging (MRI), including T<sub>2</sub> mapping and diffusion tensor imaging (DTI)<sup>6</sup>.

**Methods:** *Mice:* Experiments were conducted in adult male animals (8-16 week-old) from LysM-CRE:HIF-1 $\alpha$ <sup>fl/fl</sup> (LysM-HIF-1 $\alpha$ <sup>-/-</sup>; n=7)<sup>3</sup>, LysM-CRE:HIF-2 $\alpha$ <sup>fl/fl</sup> (LysM-HIF-2 $\alpha$ <sup>-/-</sup>; n=3)<sup>7</sup>, HIF-2 $\alpha$ <sup>fl/fl</sup> and HIF-1 $\alpha$ <sup>fl/fl</sup> (WT; n=6). *Muscle injury:* Acute muscle injury was induced by the *i.m.* injection of cardiotoxin (CTX; 50  $\mu$ l) in the tibialis anterior (TA) muscle. *MRI:* Measurements were performed before (D0) and 1 (D1), 2 (D2), 3 (D3), 7 (D7) and 21 days (D21) after the CTX injection. Investigations were performed at 11.75 T on a vertical Bruker Avance 500 MHz/89mm wide-bore imager (Bruker, Ettlingen, Germany)<sup>8</sup>. *T<sub>2</sub> mapping:* a 4-shot SE-EPI sequence was used with the following parameters: FOV: 2.0  $\times$  2.0 cm<sup>2</sup>, matrix: 128  $\times$  128, slice thickness: 1 mm, 15NEX, TR: 3500 ms, TEs ranging from 8 to 48 ms. *DTI parameters:* a segmented (4 shots) SE-EPI readout sequence was used: b-values = (0 and 450) sec/mm<sup>2</sup>; 12 diffusion-encoding directions;  $\delta/\Delta = 5/10$  ms; BW = 400 kHz; TR/TE = 3500/20 ms. *Data processing:* T<sub>2</sub> maps were generated and the DTI reconstruction was performed with the manufacturer software (Bruker; Paravision 5). DTI metrics including diffusivities ( $\lambda_1$ ,  $\lambda_2$  and  $\lambda_3$ ), apparent diffusion coefficient (ADC) and fractional anisotropy (FA) were calculated<sup>8</sup>. For both T<sub>2</sub> maps and DTI metrics, a region of interest was selected in the TA muscle. *Isolation of leukocytes and macrophages from muscle:* TA muscles were minced and digested in RPMI medium containing collagenase B 0.2% (Roche Diagnostics GmbH) at 37°C for 1h. The resulting homogenate was filtered and cells were counted. CD45<sup>+</sup> cells were isolated using magnetic sorting (Miltenyi Biotec) and stained with APC-conjugated anti-Gr1 (Ly6C/G) and PE-conjugated anti-F4/80 antibodies (eBioscience). Cells were analyzed using a FC-500 flow cytometer (Beckman Coulter). Analysis was performed with CXPTM Cytometer<sup>5</sup>. *Histological analysis:* TA muscles were removed, snap frozen in nitrogen-chilled isopentane and kept at -80°C until use. 8  $\mu$ m-thick cryosections were prepared for hematoxylin-eosin staining. Myofiber cross-sectional area (CSA) analysis was performed at D21 as recently described<sup>5</sup>. *Statistical analyses.* Two-factor analysis of variance with repeated measures on time and Newman-Keuls post-hoc analysis were used to compare MRI variables while t-tests were used for other analyses.

## Results:

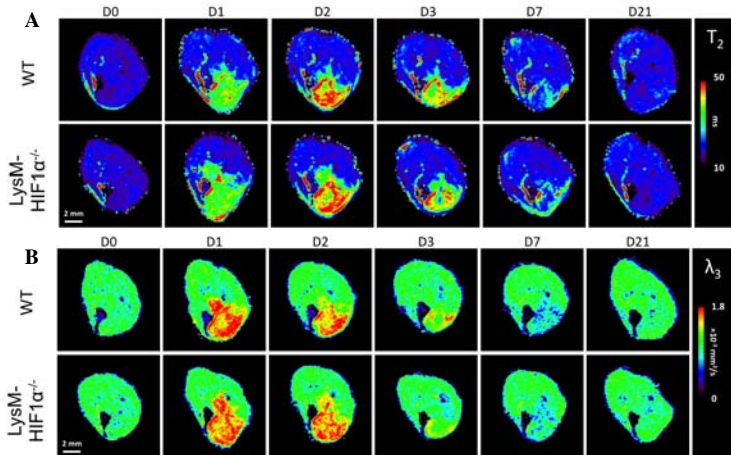


Figure 1. Typical representative axial T<sub>2</sub> maps (A) and axial maps of the third eigenvalue ( $\lambda_3$ ) (B) obtained from WT and LysM-HIF-1 $\alpha$ <sup>-/-</sup> muscles at the respective time points.

As illustrated in Figure 1, CTX injection largely modified both the DTI metrics and T<sub>2</sub> values, but these changes were strictly similar in LysM-HIF-1 $\alpha$ <sup>-/-</sup> and WT groups.  $\lambda_2$ ,  $\lambda_3$  and ADC values peaked at D1 and remained elevated at D2 and D3 as compared to baseline values (Table 1 & Figure 1). These parameters were further reduced at D7 and returned to the baseline values at D21. As compared to  $\lambda_2$  and  $\lambda_3$  changes, FA evolved in an opposite direction (Table 1). We demonstrated that the recently reported CTX-induced increase of FA at D7<sup>6</sup> was actually related to the decreased  $\lambda_2$  and  $\lambda_3$  values, reflecting the well-known presence of small-diameter regenerating muscle fibres<sup>1</sup>. The time course of CTX-induced T<sub>2</sub> changes was clearly different from that highlighted by the DTI metrics. T<sub>2</sub> values were significantly elevated at D1, peaked between D2 and D3, remained elevated at D7 and fully recovered at D21 (Figure 1). While it has been suggested that T<sub>2</sub> variations represent a marker of muscle inflammation<sup>5</sup>, T<sub>2</sub> changes may also be related to edema and/or necrosis, as illustrated by the early increase in T<sub>2</sub> values (*i.e.*, at D1). Figure 2A shows that the distribution of the two MPs subsets did not differ between the two groups during the MPs skewing period<sup>3</sup>, indicating that M1 MPs were able to skew in M2 MPs at the time of resolution of inflammation even in the absence of HIF-1 $\alpha$ . In agreement with the full recovery of MRI parameters, myofibre CSA was similar between the two groups at D21 (Figure 2B).

**Discussion:** Our multiscale methodological approach clearly demonstrated that neither HIF-1 $\alpha$  nor HIF-2 $\alpha$  (data not shown) are involved in the muscle regeneration process resulting from an acute injury. The discrepancies between our findings and those recently reported<sup>6</sup> might be related, at least in part, to the model of muscle injury (sterile injury vs. soft trauma), indicating that the lack of HIFs expression in myeloid cells might lead, at worst, to a short delay at the onset of the repair process. Overall, we concluded that myeloid HIFs are not essential for skeletal muscle regeneration and that multimodal MRI is a suitable diagnostic tool for monitoring skeletal muscle injury and repair.

**References:** <sup>1</sup>Arnold *et al. J. Exp. Med.* 2007; <sup>2</sup>Cramer & Johnson *Cell* 2003; <sup>3</sup>Peyssonnaud *et al. J. Clin. Invest.* 2005; <sup>4</sup>Scheerer *et al. J. Immunol.* 2013; <sup>5</sup>Mounier *et al. Cell Metab* 2013; <sup>6</sup>Esposito *et al. PLoS One* 2013; <sup>7</sup>Imtiyaz *et al. J. Clin. Invest.* 2010; <sup>8</sup>Gineste *et al. PLoS One* 2013.

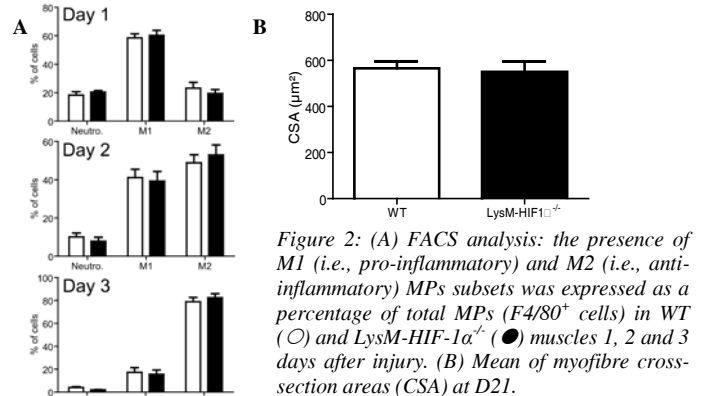


Figure 2: (A) FACS analysis: the presence of M1 (*i.e.*, pro-inflammatory) and M2 (*i.e.*, anti-inflammatory) MPs subsets was expressed as a percentage of total MPs (F4/80<sup>+</sup> cells) in WT (O) and LysM-HIF-1 $\alpha$ <sup>-/-</sup> (●) muscles 1, 2 and 3 days after injury. (B) Mean of myofibre cross-sectional areas (CSA) at D21.

		D0	D1	D2	D3	D7	D21
$\lambda_1$ ( $\times 10^3$ mm <sup>2</sup> /sec)	WT	1.77 $\pm$ 0.04	2.09 $\pm$ 0.07***	2.04 $\pm$ 0.05***	1.84 $\pm$ 0.05	1.72 $\pm$ 0.10	1.76 $\pm$ 0.04
	LysM-HIF1 $\alpha$ <sup>-/-</sup>	1.80 $\pm$ 0.07	2.08 $\pm$ 0.03***	2.05 $\pm$ 0.04***	1.80 $\pm$ 0.10	1.75 $\pm$ 0.05	1.72 $\pm$ 0.06
$\lambda_2$ ( $\times 10^3$ mm <sup>2</sup> /sec)	WT	1.30 $\pm$ 0.02	1.82 $\pm$ 0.04***	1.76 $\pm$ 0.06***	1.47 $\pm$ 0.06***	1.17 $\pm$ 0.04***	1.31 $\pm$ 0.06
	LysM-HIF1 $\alpha$ <sup>-/-</sup>	1.33 $\pm$ 0.06	1.84 $\pm$ 0.03***	1.77 $\pm$ 0.05***	1.41 $\pm$ 0.10***	1.18 $\pm$ 0.06***	1.30 $\pm$ 0.03
ADC ( $\times 10^3$ mm <sup>2</sup> /sec)	WT	1.36 $\pm$ 0.03	1.84 $\pm$ 0.03***	1.80 $\pm$ 0.05***	1.53 $\pm$ 0.06***	1.25 $\pm$ 0.06***	1.35 $\pm$ 0.04
	LysM-HIF1 $\alpha$ <sup>-/-</sup>	1.39 $\pm$ 0.05	1.83 $\pm$ 0.03***	1.81 $\pm$ 0.04***	1.46 $\pm$ 0.10***	1.28 $\pm$ 0.05***	1.34 $\pm$ 0.03
FA	WT	0.28 $\pm$ 0.01	0.14 $\pm$ 0.02***	0.13 $\pm$ 0.01***	0.19 $\pm$ 0.01***	0.34 $\pm$ 0.02***	0.29 $\pm$ 0.02
	LysM-HIF1 $\alpha$ <sup>-/-</sup>	0.28 $\pm$ 0.02	0.13 $\pm$ 0.01***	0.13 $\pm$ 0.01***	0.22 $\pm$ 0.03***	0.33 $\pm$ 0.02***	0.27 $\pm$ 0.03

Table 1: The first two eigenvalues ( $\lambda_1$  and  $\lambda_2$ ), ADC and FA values obtained from WT and LysM-HIF-1 $\alpha$ <sup>-/-</sup> muscles at the respective time points. Significantly different from values recorded at D0: \*\*\*P < 0.001.